Geophysical Research Letters

RESEARCH LETTER
10.1029/2025GL119584

Beyond Water: Mapping Sediment Bars to Enhance Satellite Monitoring of River Dynamics

Martina Cecchetto[1], Elisa Bozzolan[1], Andrea Brenna[2], Diane Doolaeghe[1], Elia Taffetani[1], Nicola Surian[1], Walter Bertoldi[3], and Simone Bizzi[1]

[1]Department of Geosciences, Università degli Studi di Padova, Padova, Italy, [2]Department of Earth Sciences "A. Desio", Università degli Studi di Milano, Milano, Italy, [3]Department of Civil, Environmental and Mechanical Engineering, University of Trento, Trento, Italy

Key Points:

- We present an automated approach to track sustained river changes using Sentinel-2 imagery classification of river water and sediment bars
- The approach separates active channel lateral mobility, widening, and narrowing from changes due to water-stage fluctuations
- Exposed sediment-to-water ratio strongly predicts channel dynamicity: sediment-rich reaches are more unstable and hydrologically responsive

Supporting Information:

Supporting Information may be found in the online version of this article.

Correspondence to:

M. Cecchetto,
martina.cecchetto@unipd.it

Citation:

Cecchetto, M., Bozzolan, E., Brenna, A., Doolaeghe, D., Taffetani, E., Surian, N., et al. (2026). Beyond water: Mapping sediment bars to enhance satellite monitoring of river dynamics. *Geophysical Research Letters*, *53*, e2025GL119584. https://doi.org/10.1029/2025GL119584

Received 23 SEP 2025
Accepted 21 DEC 2025

Author Contributions:

Conceptualization: Martina Cecchetto, Elisa Bozzolan, Andrea Brenna, Nicola Surian, Walter Bertoldi, Simone Bizzi
Data curation: Martina Cecchetto
Formal analysis: Martina Cecchetto, Elisa Bozzolan
Funding acquisition: Nicola Surian, Walter Bertoldi, Simone Bizzi
Methodology: Martina Cecchetto, Elisa Bozzolan
Project administration: Simone Bizzi
Software: Martina Cecchetto
Supervision: Nicola Surian, Walter Bertoldi, Simone Bizzi

Abstract Unvegetated sediment bars are central to river morphodynamics but are rarely used as indicators of channel dynamicity in satellite-based studies. Linking sediment dynamics and river lateral mobility requires monitoring sustained changes in both water and sediment—the active channel (AC)—to avoid stage-dependent noise. Yet, such monitoring remains rare. We introduce an automated, globally applicable approach that detects and quantifies activation (erosion) and deactivation (vegetation colonization) by tracking multi-year sustained AC directional shifts from Sentinel-2 imagery. Applied to the Po River (Italy), this approach captures trajectories across different morphologies, distinguishing lateral mobility, widening, and narrowing from changes caused by stage-dependent hydrological forcing. Results identify the exposed sediment-to-water ratio as a strong predictor of AC dynamicity, with sediment-rich reaches showing greater instability and responsiveness to hydrological variations. Our findings demonstrate that incorporating sediment areas alongside the water channel improves understanding of river dynamics, with implications for river restoration and risk mitigation.

Plain Language Summary Bare, exposed patches of sediment that appear in rivers play an important role in how rivers change shape and behave over time. To test whether sediment can serve as a proxy for river mobility, it is necessary to track both flowing water and adjacent unvegetated sediment bars—the active channel—and to distinguish short-lived fluctuations from sustained changes over time. This study combines satellite imagery and machine learning to automatically map areas progressively gained through bank erosion or lost through vegetation colonization. By focusing on spatiotemporal sustained changes, this approach distinguishes active channel changes caused by lateral mobility from those resulting from sustained low- or high-water stages (e.g., during droughts). When applied to the Po River in Italy, the analysis showed that river segments with a higher proportion of exposed sediment relative to water show greater responsiveness to hydrological variations. This exposed sediment-to-water ratio emerges as a useful indicator of river sensitivity to change, likely because it reflects both natural channel characteristics and the legacy of past human interventions. The proposed approach offers a practical tool for global river monitoring in support of climate adaptation, river restoration projects, and flood risk mitigation strategies.

1. Introduction

Interest is growing in assessing and visualizing the extent of rivers lateral mobility to help shift perspectives toward granting rivers greater freedom (McCabe et al., 2025; Piégay et al., 2005). Mobility originates from erosion of vegetated banks and sediment bars, accretion of bars, and channel bars migration (Chadwick et al., 2023; Langhorst & Pavelsky, 2023). Therefore, assessing river mobility requires frequent monitoring (Donovan & Belmont, 2019; Ziliani & Surian, 2012) not only of flowing water but also of unvegetated sediment bars—that is, of the entire active channel area (O'Connor et al., 2003).

Advances in remote sensing technologies and (semi-) automatic classification methods are now making this possible. In particular, these advances have enabled a shift from monitoring only water-channel changes (Allen & Pavelsky, 2018; Boothroyd et al., 2021; Filipponi et al., 2025; Greenberg et al., 2024; Leenman et al., 2023; Li & Limaye, 2025; Pavelsky & Smith, 2008; Pekel et al., 2016) to mapping the entire active channel (Boothroyd et al., 2020; P. E. Carbonneau et al., 2020; Henshaw et al., 2013; Lamichhane et al., 2025; Monegaglia et al., 2018; Nyberg et al., 2023; Rowland et al., 2016; Schwenk et al., 2017; Sutfin et al., 2020).

Validation: Martina Cecchetto, Elisa Bozzolan, Diane Doolaeghe, Elia Taffetani
Visualization: Martina Cecchetto
Writing – original draft: Martina Cecchetto
Writing – review & editing: Martina Cecchetto, Elisa Bozzolan, Andrea Brenna, Nicola Surian, Simone Bizzi

To automatically monitor mobility over time, satellite-based approaches typically compare the active channel area from year to year (Rowland et al., 2016; Rusnák et al., 2025). This approach, however, has two main drawbacks. First, without thorough visual checks, it might retain spurious changes that are not geomorphologically meaningful but instead reflect classification errors–an issue that becomes more relevant in short time observation windows (Donovan et al., 2019). Second, it challenges the distinction between changes caused by active channel lateral mobility and transient changes mostly driven by prolonged water-stage variations. For instance, prolonged droughts and subsequent floods can alternately reduce or expand active channel areas through vegetation encroachment and removal on sediment bars (Bertoldi et al., 2011).

These transient, water-stage dependent changes, though geomorphologically relevant, often do not reflect true channel mobility or progressive narrowing and widening. No studies analyzing active channel changes have attempted to separate meaningful planform changes that shape a river's evolutionary trajectory from spurious changes due to inaccurate channel delineation or transient changes driven by water-stage variations. Attempts were only made in the analysis of the water channel (e.g., Leenman et al., 2023). Yet, this distinction is crucial also in active channel analyses if we want to unlock the complex feedbacks between channel morphology and active channel mobility (Chadwick et al., 2025; Kleinhans & Van Den Berg, 2011).

Channel morphology, in turn, is mediated by sediment bars (Church & Rice, 2009; Egozi & Ashmore, 2008). There is evidence that sediment bars, acting as both sources and sinks of material, directly influence river sensitivity to disturbance (Fryirs, 2017) as they drive channel morphology and processes (Church, 2006; Rice et al., 2009). Sediment bars serve as valuable indicators of river evolutionary trajectory (Llena et al., 2020; Surian, 1999) and proxies of changes in sediment transport (Brenna et al., 2022) as a consequence of river regulation (Holušová & Galia, 2025; Hu et al., 2024). In satellite-based studies, most efforts have focused either on mapping the morphology and evolution of bars as proxies for bedload sediment transport and the impacts of river regulation (e.g., Kryniecka et al., 2022; Wang & Xu, 2018) or on assessing river lateral mobility by aggregating water and sediment extents (e.g., Boothroyd et al., 2020; Schwenk et al., 2017). These two research lines have rarely intersected. Here, we integrate both by using combined and disaggregated information from water and exposed sediment units within the active channel to better link and understand channel morphology and dynamics.

The objectives of this work are to: (a) apply a novel pixel-based tracking method to detect multi-year shifts of the active channel and isolate sustained lateral changes as proxies of mobility; and (b) explore the functional relationships between spatiotemporal variability of these sustained active channel changes and channel morphological metrics. Spanning 2017 to 2024, we apply the approach to the Po River (Italy), to prove its consistency to different channel morphologies under the legacy of human-induced alterations. We find that the extent of exposed sediment area constraints the active channel change patterns, thereby connecting river planform dynamism with new satellite-derived morphological metrics. Given that the active channel masks are generated from a freely accessible, global Sentinel-2-based Fully Convolutional Network (FCN; P. E. Carbonneau and Bizzi, 2024), the proposed approach is potentially transferable to any location.

2. Methodology

2.1. Study Area Settings

At 651 km, the Po River is Italy's longest watercourse (Brenna et al., 2022). Its strategic location and dense human settlement have led to significant anthropogenic alterations, particularly since the mid-20th century (Brenna et al., 2024; De Sordi et al., 2025). Measures to promote navigability—combined with in-channel mining, deforestation, decreased tributary sediment supply, and the 1962 construction of the Isola Serafini Dam (Figure 1a)—altered sediment flux and reduced the river's morphological complexity and dynamicity (Nones et al., 2024). Though direct human pressure has eased, its legacy persists (Boothroyd et al., 2021; Brenna et al., 2022; De Sordi et al., 2025; Maselli et al., 2018).

On top of that, over the past two decades, summer streamflow in the Po River has declined (Nones et al., 2024) as a result of snow accumulation deficit during winters aggravated by climate change, greater evapotranspiration during dry and hot summers, and increased irrigation withdrawals (Avanzi et al., 2024). The 2022 drought, for example, marked a six-century return period (Montanari et al., 2023). These pressures make the Po River an

10.1029/2025GL119584

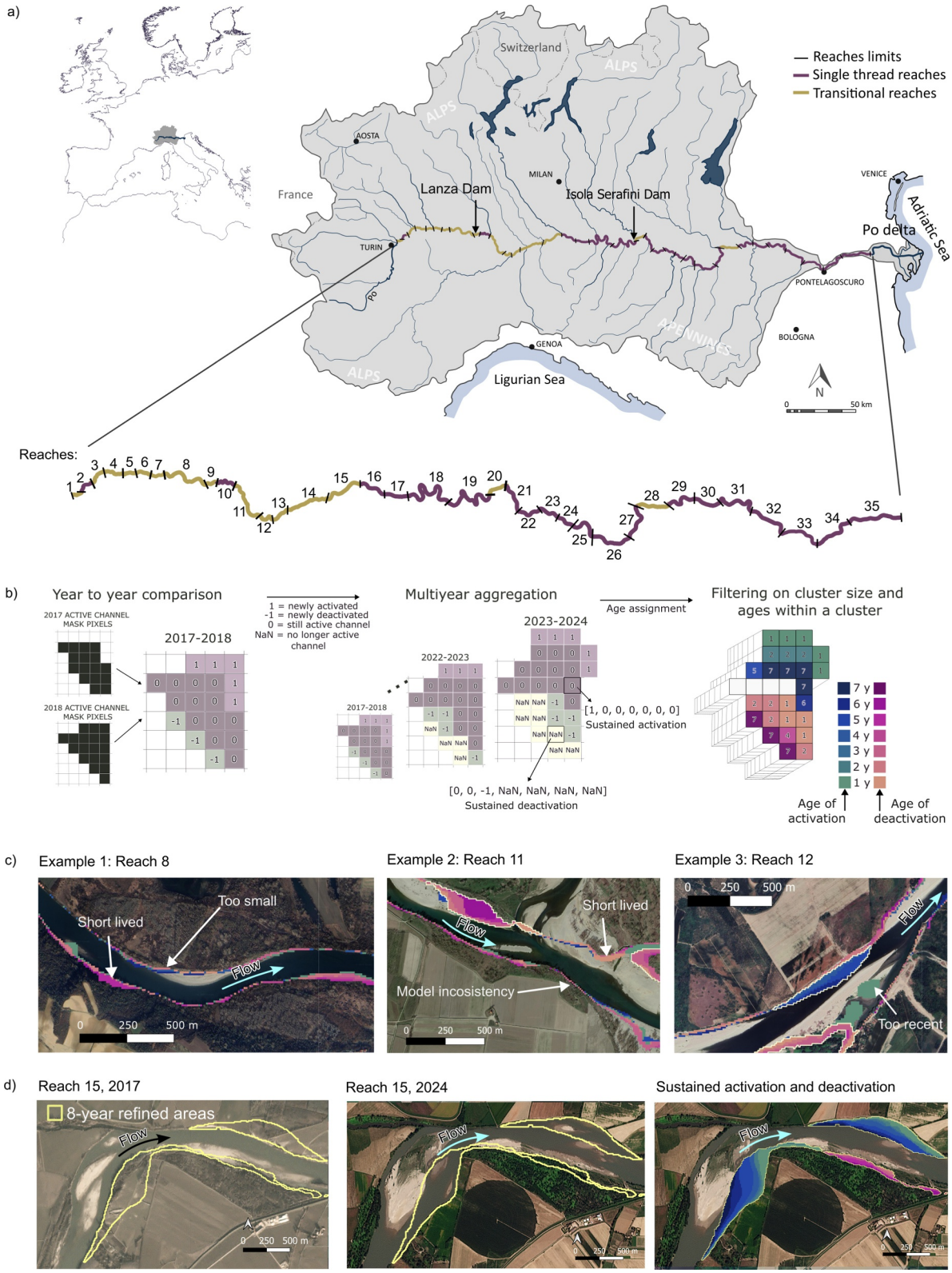

Figure 1. (a) Map of the analyzed Po River course, divided into transitional (gold) and single-thread (burgundy) reaches. (b) Workflow: annual AC masks are compared to map activated, deactivated, and unchanged areas; multi-year aggregation isolates sustained changes; pixels are filtered by size and temporal consistency. (c) Examples of automatically excluded areas due to small size, lack of progressive change, model inconsistency, or final-year change only. (d) Refined areas (light yellow polygons) and yearly sustained AC changes over Planet imagery for reach 15 (2017–2024).

exemplary case study for assessing river sensitivity to climate change and new management interventions, such as restoration projects.

The study area spans 500 km from the Stura di Lanzo confluence to the Po di Goro intake marking the beginning of the deltaic area (Figure 1a). It includes 35 geomorphologically homogeneous reaches, grouped as either transitional or single-thread (Figure 1a; Table S1 in Supporting Information S1). This classification is primarily based on two standard indices, the sinuosity and the braiding indices, measured from single high-resolution image (Egozi & Ashmore, 2008; Rinaldi et al., 2016). Reaches are also denoted by a percentage of anthropogenic confinement (Fryirs et al., 2016) which De Sordi et al. (2025) computed by mapping the fraction of river channel margins with anthropic structures that can limit lateral mobility (Table S1 in Supporting Information S1).

2.2. Active Channel Classification From Satellite Imagery

The source of satellite imagery used in this study is the Sentinel-2 Level 2A products (hereafter S2). With a revisit time of 5 days and a resolution of 10 m for spectral bands B3, B4, and B8 (i.e., Green, Red and Near InfraRed), S2 imagery is suitable for mapping water channel and exposed sediment bars in rivers comparable in size to the Po River (Bozzolan et al., 2023).

The processing pipeline is detailed in Supporting Information S1. Briefly, for each month from January 2017 to December 2024, monthly median composite images were generated using spectral bands B3, B4, and B8 from S2 scenes with less than 85% cloud cover. Monthly composites were processed with an FCN-based algorithm that classifies lake water, river water, and sediment bars using spectral, shape, and texture features (P. E. Carbonneau & Bizzi, 2024). When tested on the Po River against a 0.3 m orthophoto, river water was detected with over 90% accuracy, while sediment classification exceeded 70%, aligning with global benchmarks (Bozzolan et al., 2026). By aggregating pixels classified as river water with adjacent sediment bars, a mask of the active channel, hereafter AC, is produced for each month.

Temporal aggregation of monthly data into annual AC maps requires careful consideration. In satellite-based geomorphic analysis, the median annual composite is generally assumed to help dampen intra-annual river stage variability in AC classification (Boothroyd et al., 2020; Nyberg et al., 2023). This study, instead, adopts the method from Bozzolan et al. (2026) who demonstrated that aggregating monthly AC masks into annual water and sediment frequency maps captures intra-annual dynamics more effectively, while reducing monthly classification errors and biases arising from mixed pixels. Pixels classified as either river water or exposed sediment bars for at least 4 months/year define the annual AC, balancing model accuracy and geomorphic dynamics across different channel morphologies (see details in Supporting Information S1 and in Bozzolan et al., 2026). The final AC mask is then manually checked to remove areas not relevant for the present analysis, such as tributaries confluence parts.

Yearly water and sediment frequency maps are also used to compute the 8-year average exposed sediment-to-water area ratio, R_{sw}, per reach (Figure S3 in Supporting Information S1). The sediment areas for the ratio were defined as all pixels classified as sediment at least once per year, with the remaining pixels aggregated into the water extent.

2.3. Pixel-Based Reconstruction of Sustained Active Channel Changes

Yearly AC binary masks were used to automatically track the evolution of each pixel ever classified as part of the AC during the 8-year period. Each yearly mask was compared to the subsequent one: pixels classified as part of the AC in both years were assigned a value of 0, while those that became part of the active channel (i.e., activated) were labeled 1, and -1 was assigned to those that were excluded (i.e., deactivated) (Figure 1b). Pixels located outside consecutive AC masks were given NaN (Not a Number) labels. When interannual information was aggregated along the multiyear domain, it was possible to track state changes in pixel's classification over time in relation to the river AC. For example, the 2017–2024 temporal sequence [1, 0, 0, −1, NaN, NaN, NaN] indicates pixel activation in 2018, sustained through 2020, deactivation in 2021, and not active afterward.

This data set formed the basis for refining sustained channel changes and locate lateral mobility over time. Pixels were grouped as activated or deactivated if change was sustained over the studied time span. The former are sequences starting with 1 followed by only 0s (e.g., [NaN, 1, 0, 0, 0, 0, 0]), indicating sustained inclusion in the AC; the latter start with −1 and continue with NaNs, reflecting long-term exclusion. The position of the 1 or -1

defines the "age" of activation/deactivation (e.g., 6 years in the example), that is, the duration of the sustained change. Adjacent pixels with the same class (activation or deactivation) were merged into clusters (Figure 1b).

To focus on meaningful spatial trends, two filters were applied. First, based on the cumulative frequency distribution of clusters size, categorized by the number of ages they contain (Figure S4 in Supporting Information S1), we retained only clusters with at least 4 years of sustained, coherent changes, thus discarding transient ('short lived' or 'model inconsistency' in Figure 1c) or recent changes ('too recent' in Figure 1c). Second, the remaining clusters smaller than the 75th percentile of the size distribution (Figure S4 in Supporting Information S1) were excluded based on expert judgment ('too small' in Figure 1c). We sense-checked the resulting data set containing the automatically refined planform change areas on QGIS with high-spatial resolution images from Planet constellation (https://www.planet.com), see Figure 1d.

2.4. Factors Influencing Active Channel Changes

For each reach, activated and deactivated areas were normalized by the AC area to compute A*. Their difference gives the net change, and their sum the total planimetric change, A^*_{TOT}. We assessed the influence of channel morphology, artificial confinement, AC width, AC width normalized by the drainage area, and channel slope in driving sustained, geomorphologically significant changes of the AC. In addition to these commonly used metrics, we tested the exposed sediment-to-water ratio, R_{sw}, which is directly derived from the classifier outputs and thus available without requiring additional source of information. To assess the influence of hydrology, we used daily water-discharge records from the Pontelagoscuro gauging station (https://www.arpae.it/, Figure 1a) to calculate total annual discharge volume, which we adopted as the representative hydrological metric.

3. Results

Applied to the Po River, the automated procedure identified geomorphic changes sustained over the past 8 years, while excluding transient, water-stage–driven changes and spurious variations caused by inaccurate automatic delineation. Figure 1d illustrates an example of such refined changes, showing localized bank erosion and gradual AC abandonment due to vegetation encroachment in reach 15, confirmed using 3 m resolution images of 2017 and 2024 from Planet constellation. After visual checks, what remains as valid areas mostly reflect progressive river lateral mobility. Discarded areas typically identify either negligible morphological dynamics (Example 1, Figure 1c), changes appeared only in the final year, leaving their continuation uncertain (Example 3, Figure 1c), or classification noise—commonly at the AC margins, where overhanging vegetation and mixed spectral signature around pioneering vegetation introduce inter-annual variability in AC delineation (Example 2, Figure 1c) as assessed in Bozzolan et al. (2026).

3.1. Po River Geomorphic Changes

Figure 2a shows three examples of trajectory evolution in relation to bank protection works, high channel dynamism, and a restoration intervention. In Reach 6, lateral mobility due to intense erosion along the left bank has progressed up to the artificial boundaries formed by bank protection structures. This suggests that future erosion may slow as the channel reaches its confinement limit, potentially enabling reactivation of the opposite, true-right riverbank now still inactive. In contrast, Reach 14 (36% artificial confinement) shows extensive activation, including secondary channel reactivation and major bank erosion. Reach 28 exhibits activation comparable to less confined reaches. This response is likely linked to a 2013 intervention that lowered a diversion groyne, triggering progressive erosion along a former secondary channel.

When changes are aggregated by reach (plot in Figure 2a), the pronounced dynamicity and dominance of activation in Reach 14 become evident, as does the distinct behavior of Reach 28 compared to its neighboring reaches. In contrast, Reach 6 shows a near-equilibrium between activation and deactivation, manifested as a lateral shift of the AC. In the Po River upstream part, net changes suggest some reaches are dynamically stable (e.g., Reach 5, 6, and 13), while others are widening (Reach 3, 11, 12, 14, and 15), supporting earlier findings of planimetric stability or recovery to wider channel configuration in this area (Brenna et al., 2022; De Sordi et al., 2025). This trend reverses in Reaches 7 to 10 and 16 to 24 (with the exception of 20), located near the Lanza Dam and Isola Serafini Dam, respectively. Here, deactivation exceeds activation, indicating that the ongoing loss of AC areas is not being compensated by new channel areas. This is consistent with the narrowing process previously documented in these sectors of the river (Brenna et al., 2022; De Sordi et al., 2025).

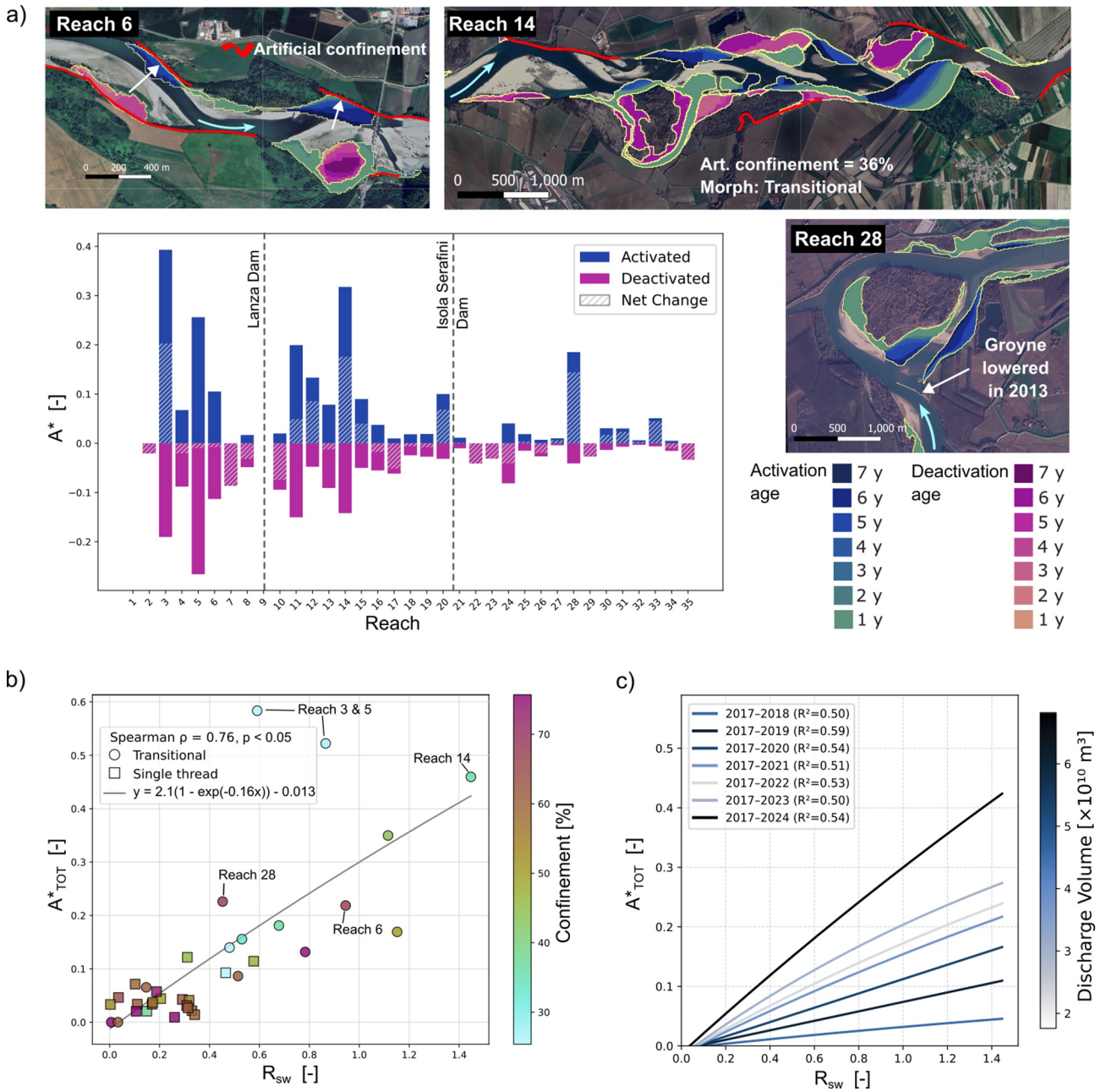

Figure 2. (a) 8-year cumulative normalized areas of change, A*—activation and deactivation (plotted as negative for visualization)— along the Po River, and their net balance with examples of sustained activation and deactivation in three reaches influenced by artificial confinement (Reach 6 and 14) and a restoration intervention (Reach 28). (b) A^*_{TOT} over the 8-year period plotted against R_{sw} for each reach, grouped by morphology and artificial confinement. (c) Asymptotic relationships between A^*_{TOT} and R_{sw}. Blue lines represent asymptotic fits, with respective R^2, based on progressively longer time windows. Darker blue shades indicate higher annual discharge volumes.

3.2. Drivers of Active Channel Changes

We show that AC changes (A^*_{TOT}) over the 8-year period are unrelated to reaches AC width and slope (Figure S5 in Supporting Information S1). In contrast, A^*_{TOT} correlates moderately with AC width normalized by the drainage area (Spearman's $\rho = 0.57$, $p < 0.05$). Channel morphology shows a positive correlation ($\rho = 0.61$, $p < 0.05$), indicating that reaches with higher braiding indexes (Rinaldi et al., 2016) are more dynamic ($\rho = 0.56$, $p < 0.05$). Artificial confinement, by contrast, moderately limits lateral mobility ($\rho = -0.49$, $p < 0.05$). The strongest relationship is, instead, with R_{sw} ($\rho = 0.76$, $p < 0.05$). As shown in Figure 2b, normalized area of change

A^*_{TOT} over 8 years increases with this ratio. Using an asymptotic curve, $R^2 = 0.54$ (alternative curves in Figure S6 in Supporting Information S1), we identify R_{sw} as the dominant control on channel changes.

We disaggregated the 8-year data set to compute the reaches' annual extent of activated and deactivated A* (Figure S7 in Supporting Information S1). An asymptotic relationship was then tested across progressively increasing time windows (from 2017 to 2024), with the corresponding R^2 values shown in Figure 2c for the A^*_{TOT} per reach. The association between lateral mobility and R_{sw} remained consistent across progressively increasing time windows, with R^2 values always exceeding 0.50.

Starting from 2017 and incrementally extending the time window, it becomes possible to assess how the different years contributed to the river adjustment. Results indicate that reaches with a higher proportion of exposed sediment relative to water tend to show greater responsiveness to hydrological variations. Hydrological forcing is illustrated by line color, with darker blues indicating higher total annual discharge volume. Morphological effectiveness is evident in 2019, 2020, and especially 2024, all years of high discharge volume, whereas the driest years 2022 and 2023 showed only limited changes.

4. Discussion

Using an automated pixel-based reconstruction of the river AC evolution, we show that incorporating sediment bars provides new insights into various river mobility processes. Traditional metrics—such as type of morphology (Greenberg et al., 2024), AC width and slope (Boothroyd et al., 2025), or AC width normalized by drainage area (Alber & Piégay, 2017)— only weakly or moderately predict mobility. Instead, we identify the exposed sediment-to-water ratio, R_{sw}, as the most effective indicator of geomorphic AC change.

Mobility is a consequence of time-dependent interactions between water reshaping the land (through bank erosion and bars accretion) and vegetation colonizing and stabilizing sediment bars (Corenblit et al., 2024). R_{sw} integrates the water–sediment–vegetation interplay and explicitly reflects variability both between and within channel morphologies. Unlike conventional morphological indexes (e.g., Rinaldi et al., 2016), this ratio is not derived from a single-date imagery. It overcomes the limitations of static, condition-sensitive classification indexes (e.g., Egozi & Ashmore, 2008), whose link to mobility, as shown here and by Boothroyd et al. (2025), is not always consistent.

This ratio complements and integrates information from confinement. Confinement constrains lateral migration, reducing space available for bar formation and sediment reworking (Greenberg et al., 2024). As a result, the extent of exposed sediment not only measures channel activity but also preserves evidence of natural and human-induced pressures (Dong et al., 2024; Holušová & Galia, 2025; Hooke & Yorke, 2011). In the Po River, as in many rivers worldwide (Grill et al., 2019), anthropogenic pressures have, over recent decades, promoted vegetation colonization at the expense of exposed sediment bars, leading to morphological simplification and reduced lateral mobility (Boothroyd et al., 2021; Brenna et al., 2022, 2024; Maselli et al., 2018). However, confinement should be interpreted relative to the river's migration trajectory during the observation period. This explains why Reaches 3 and 5 deviate from the asymptotic fit (Figure 2b): limited confined margins outside the migrating zone allow extensive bank erosion. Reach 6 illustrates another example: despite 66% artificial confinement, it remained highly mobile until activation reached the bank protections (Figure 2a), indicating potential future effects on AC configuration and mobility.

Given the relatively short time span, R_{sw} was here averaged over the 8-year period. Tracking its temporal evolution can, however, reveal shifts in river functioning or type not evident from AC masks alone. Its updatable nature and broad applicability should be further evaluated across different river systems. This updatable nature also characterizes our approach to assessing directions of lateral mobility. By monitoring and clustering changes over multiple years rather than on a year-by-year basis (e.g., Rusnák et al., 2025), we could separate water-stage–driven variability from sustained morphological changes, often proxy of progressive lateral mobility.

To demonstrate this, we performed two analyses: one spanning 2017–2023 (Figure 3a) and another including 2024 (Figure 3b). Figures 3a and 3b show annual activation and deactivation trends alongside discharge data. If the analysis were limited to 2023, the data would highlight significant deactivation during the dry years of 2021 and 2022. With a total discharge volume comparable to that of 2021 (3.1 and $3.6 \bullet 10^{10}$ m^3, respectively), deactivation in 2023 remains higher than activation, though it declined, likely due to late-year flood events (Figure 3a). However, the inclusion of 2024—a hydrologically intense year with the highest discharge volume in the 8-year

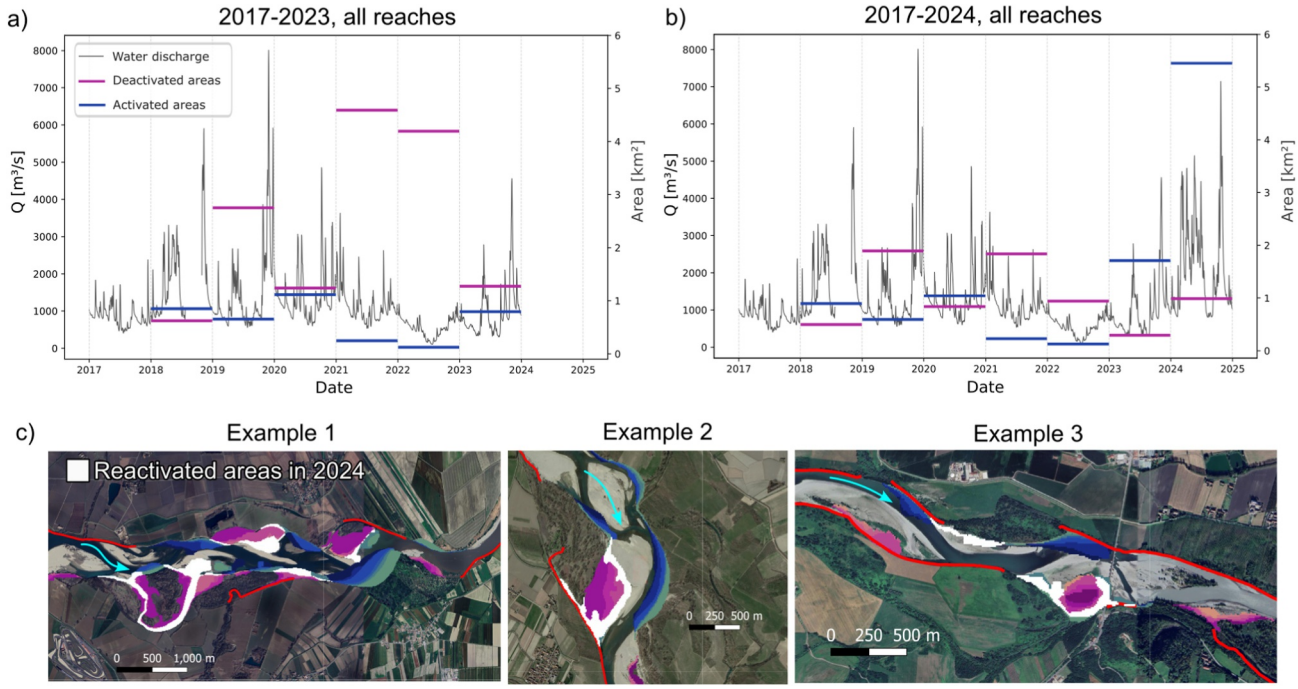

Figure 3. Daily discharge at Pontelagoscuro for 2017–2023 (a) and 2017–2024 (b), with total activated and deactivated areas across all reaches of the Po River (secondary *y*-axis) overlaid for the year of occurrence. (c) Examples of previously deactivated areas reactivated in 2024. Light blue arrows and red lines indicate flow direction and artificially confined margins, respectively.

record ($6.8 \bullet 10^{10}$ m^3) and the sixth highest annual flow volume in 100-year record—reveals widespread reactivation of previously abandoned areas, particularly those deactivated in the prior three dry years. This suggests that those changes were not geomorphologically persistent (i.e., due to river mobility) but rather caused by prolonged low water stages that favored colonization by pioneering vegetation on sediment bars.

In 2024, the river reoccupied nearly 40% of areas deactivated in 2023, 34% of 2022%, and 26% of 2021. In contrast, areas lost in 2018–2020 showed only limited recovery (~13%). As shown in Figure 3c, reactivations mainly occurred in secondary channels, near-wetted channel zones, or areas overgrown by early-stage vegetation during the low-flow period. Conversely, the addition of 2024 had minimal impact on previous activated areas, except for 2023, where disconnected patches became part of larger activation zones. Whether the major reactivations observed in 2024 represent a lasting change remains to be assessed by extending the time series over the coming years. Our automated monitoring approach allows for such extension, enabling consistent validation of planform changes and improving the robustness of trajectory assessments.

While a quantitative analysis of hydrological controls on AC sensitivity lies beyond the scope of this study, a qualitative relationship emerges in Figures 2c and 3b. Using the AC change, we can estimate the river response and recovery to hydrological extremes. The hydrological events of 2024 followed a prolonged period of reduced flows, a pattern increasingly observed in the Po River basin, likely influenced by climate change (Avanzi et al., 2024). The alternation of extreme conditions, hence the intensification in discharge variability, has increased the pace of channel activation (Leenman et al., 2025). Breaking down the 8-year changes into annual AC modifications helps relate the river's response to successive hydro-climatic extremes and support unraveling the interplay between hydrology and river morphology.

Given the societal and ecological implications of letting rivers more room to move (McCabe et al., 2025), a self-updating monitoring approach of rivers AC is crucial also in river management (Brierley & Fryirs, 2016; Piégay et al., 2005). Sustained activation and deactivation can be used to assess the impact of (and on) bank protections, compute bank retreat rate (Nardi et al., 2013), as well as sediment and carbon sources and sinks (Geyman et al., 2025; Greenberg et al., 2024) at both network and reach scales. With the proposed approach, activation, deactivation, and exposed sediment-to-water ratio can be assessed globally. Its applicability using S2 data is

generally limited to medium- and large rivers with active channel widths greater than ~50 m, where classification accuracies are robust (Bozzolan et al., 2023).

The approach presented here was developed for annually resolved morphological changes and may not fully capture intra-annual or event-driven changes (Rowland et al., 2016). However, the pixel-based reconstruction of sustained changes could be adapted for monthly-scale monitoring or for sequences of consecutive Sentinel-2 images, improving understanding of the river's sensitivity to drivers. The approach emphasizes progressive planform changes, thereby filtering out intermittent changes that can occur in laterally dynamic rivers between years (e.g., areas changing from active 1 year to inactive the following years and back to active the years after). What constitutes sustained changes (in terms of temporal sequence and spatial extent) can, however, be tuned depending on river specific dynamics, such as modifying the number of sequential years required for change detection (set to 4 years in this study). Future developments should include the monitoring of geomorphic processes within the AC boundaries, such as sediment bar evolution, water-channel mobility, or channel-thread reconfiguration; while this aspect is probably less relevant for a management prospective, combining these processes with AC planform changes could help define feedbacks between channel morphology and mobility.

5. Conclusions

We developed an automated approach to detect spatiotemporally sustained changes in river AC from satellite imagery. Applied to the Po River (2017–2024), the approach revealed that:

1. Pixel-based history of AC changes effectively filters spurious or transient changes, obtaining robust assessment of AC lateral mobility at 10 m resolution, scalable to medium- and large rivers worldwide across diverse morphologies.
2. The exposed sediment-to-water ratio is a strong predictor of river sensitivity to changes; reaches with larger sediment proportions show a greater mobility and higher responsiveness to hydrological variations.
3. Accounting for sediment bars alongside water improves understanding of river dynamics, specifically of planform changes, with direct implications for river restoration and risk mitigation.

Together, these findings highlight the potential of combining satellite-observed river changes and satellite-derived metrics to advance global monitoring of river dynamics and to uncover key drivers of fluvial geomorphic change.

Conflict of Interest

The authors declare no conflicts of interest relevant to this study.

Data Availability Statement

The S2 images used for the analysis are open-source and are available in https://browser.dataspace.copernicus.eu. The FCN model to classify S2 monthly medians is available in P. Carbonneau (2023) and is described in P. E. Carbonneau and Bizzi (2024). The active channel masks are available in Bozzolan (2025), and the activation and deactivation maps can be downloaded from Cecchetto (2025).

Acknowledgments
We would like to thank the editor, one anonymous reviewer, and prof. Yong Hu for their constructive reviews.
This work was primarily funded through the project 'Green Rivers' PRIN PNRR 2022 (MUR P20229WTX7, CUP "C53D23010160001"). Other co-authors benefited from funding sources from the project 'River Watching' PRIN 2022 (MUR 20223RXTHB, CUP "C53D23001930006") and the research project PARACELSO funded by ASI and coordinated by the river Po Water Authority. This work was also undertaken as part of the Project "The Geosciences for Sustainable Development" [CUP C93C23002690001]. The scientific colour map used in some figures refers to Crameri et al. (2020). Open access publishing facilitated by Universita degli Studi di Padova, as part of the Wiley - CRUI-CARE agreement.

References

Alber, A., & Piégay, H. (2017). Characterizing and modelling river channel migration rates at a regional scale: Case study of south-east France. *Journal of Environmental Management*, *202*, 479–493. https://doi.org/10.1016/j.jenvman.2016.10.055

Allen, G. H., & Pavelsky, T. M. (2018). Global extent of rivers and streams. *Science*, *361*(6402), 585–588. https://doi.org/10.1126/science.aat0636

Avanzi, F., Munerol, F., Milelli, M., Gabellani, S., Massari, C., Girotto, M., et al. (2024). Winter snow deficit was a harbinger of summer 2022 socio-hydrologic drought in the Po Basin, Italy. *Communications Earth & Environment*, *5*(1), 64. https://doi.org/10.1038/s43247-024-01222-z

Bertoldi, W., Drake, N. A., & Gurnell, A. M. (2011). Interactions between river flows and colonizing vegetation on a braided river: Exploring spatial and temporal dynamics in riparian vegetation cover using satellite data. *Earth Surface Processes and Landforms*, *36*(11), 1474–1486. https://doi.org/10.1002/esp.2166

Boothroyd, R. J., Nones, M., & Guerrero, M. (2021). Deriving planform morphology and vegetation coverage from remote sensing to support River management applications. *Frontiers in Environmental Science*, *9*, 657354. https://doi.org/10.3389/fenvs.2021.657354

Boothroyd, R. J., Williams, R. D., Hoey, T. B., Barrett, B., & Prasojo, O. A. (2020). Applications of google Earth engine in fluvial geomorphology for detecting river channel change. *WIREs Water*, *8*(1), e21496. https://doi.org/10.1002/wat2.1496

Boothroyd, R. J., Williams, R. D., Hoey, T. B., Brierley, G. J., Tolentino, P. L. M., Guardian, E. L., et al. (2025). Big data show idiosyncratic patterns and rates of geomorphic river mobility. *Nature Communications*, *16*(1), 3263. https://doi.org/10.1038/s41467-025-58427-9

Bozzolan, E. (2025). Enhancing active channel delineation in Alluvial Rivers using monthly aggregation of Sentinel-2 imagery (version v0). *Zenodo*. https://doi.org/10.5281/ZENODO.16037537

Bozzolan, E., Brenna, A., Surian, N., Carbonneau, P., & Bizzi, S. (2023). Quantifying the impact of spatiotemporal resolution on the interpretation of fluvial geomorphic feature dynamics from sentinel 2 imagery: An application on a braided River reach in Northern Italy. *Water Resources Research*, *59*(12), e2023WR034699. https://doi.org/10.1029/2023WR034699

Bozzolan, E., Matteligh, E., Brenna, A., Cecchetto, M., Surian, N., Carbonneau, P., & Bizzi, S. (2026). Enhancing active channel delineation in alluvial Rivers using monthly aggregation of Sentinel-2 imagery. *Earth and Space Science*, *13*(1), e2025EA004642. https://doi.org/10.1029/2025EA004642

Brenna, A., Bizzi, S., & Surian, N. (2022). A width-based approach to estimating historical changes in coarse sediment fluxes at river reach and network scales. *Earth Surface Processes and Landforms*, *47*(10), 2560–2579. https://doi.org/10.1002/esp.5395

Brenna, A., Bizzi, S., & Surian, N. (2024). How multiple anthropic pressures may lead to unplanned channel patterns: Insights from the evolutionary trajectory of the Po River (Italy). *Catena*, *234*, 107598. https://doi.org/10.1016/j.catena.2023.107598

Brierley, G. J., & Fryirs, K. A. (2016). The use of evolutionary trajectories to guide 'Moving Targets' in the management of River futures. *River Research and Applications*, *32*(5), 823–835. https://doi.org/10.1002/rra.2930

Carbonneau, P. (2023). *Semantic_Classification_of_Rivers_and_Bars* (Version v1.3) [Computer software]. *Zenodo*. https://doi.org/10.5281/ZENODO.10016467

Carbonneau, P. E., & Bizzi, S. (2024). Global mapping of river sediment bars. *Earth Surface Processes and Landforms*, *49*(1), 15–23. https://doi.org/10.1002/esp.5739

Carbonneau, P. E., Dugdale, S. J., Breckon, T. P., Dietrich, J. T., Fonstad, M. A., Miyamoto, H., & Woodget, A. S. (2020). Adopting deep learning methods for airborne RGB fluvial scene classification. *Remote Sensing of Environment*, *251*, 112107. https://doi.org/10.1016/j.rse.2020.112107

Cecchetto, M. (2025). Activation and deactivation maps of the Po River (Italy), spanning 2017 to 2024 [Dataset]. *Zenodo*. https://doi.org/10.5281/ZENODO.17182742

Chadwick, A. J., Greenberg, E., & Ganti, V. (2023). Remote sensing of riverbank migration using particle image velocimetry. *Journal of Geophysical Research: Earth Surface*, *128*(7), e2023JF007177. https://doi.org/10.1029/2023JF007177

Chadwick, A. J., Greenberg, E., & Ganti, V. (2025). Single- and multithread rivers originate from (im)balance between lateral erosion and accretion. *Science*, *389*(6756), 146–150. https://doi.org/10.1126/science.ads6567

Church, M. (2006). Bed material transport and the morphology of alluvial river channels. *Annual Review of Earth and Planetary Sciences*, *34*(1), 325–354. https://doi.org/10.1146/annurev.earth.33.092203.122721

Church, M., & Rice, S. P. (2009). Form and growth of bars in a wandering gravel-bed river. *Earth Surface Processes and Landforms*, *34*(10), 1422–1432. https://doi.org/10.1002/esp.1831

Corenblit, D., Piégay, H., Arrignon, F., González-Sargas, E., Bonis, A., Ebengo, D. M., et al. (2024). Interactions between vegetation and river morphodynamics. Part II: Why is a functional trait framework important? *Earth-Science Reviews*, *253*, 104709. https://doi.org/10.1016/j.earscirev.2024.104709

Crameri, F., Shephard, G. E., & Heron, P. J. (2020). The misuse of colour in science communication. *Nature Communications*, *11*(1), 5444. Article 1. https://doi.org/10.1038/s41467-020-19160-7

De Sordi, M. V., Vezzoli, G., & Brardinoni, F. (2025). Limits to fluvial planimetric adjustment imposed by anthropogenic confinement. *Catena*, *254*, 108908. https://doi.org/10.1016/j.catena.2025.108908

Dong, C., Feng, M., Jing, H., & Yang, R. (2024). The impact of changes in water–sediment relationships at river confluences on the evolution of river bars. *Journal of Hydrology*, *645*, 132212. https://doi.org/10.1016/j.jhydrol.2024.132212

Donovan, M., & Belmont, P. (2019). Timescale dependence in river channel migration measurements. *Earth Surface Processes and Landforms*, *44*(8), 1530–1541. https://doi.org/10.1002/esp.4590

Donovan, M., Belmont, P., Notebaert, B., Coombs, T., Larson, P., & Souffront, M. (2019). Accounting for uncertainty in remotely-sensed measurements of river planform change. *Earth-Science Reviews*, *193*, 220–236. https://doi.org/10.1016/j.earscirev.2019.04.009

Egozi, R., & Ashmore, P. (2008). Defining and measuring braiding intensity. *Earth Surface Processes and Landforms*, *33*(14), 2121–2138. https://doi.org/10.1002/esp.1658

Filipponi, F., Colazzo, G., Vassoney, E., Comoglio, C., & Filippa, G. (2025). Sentinel-2 reveals record-breaking Po River shrinking due to severe drought in 2022. *Remote Sensing*, *17*(6), 1070. https://doi.org/10.3390/rs17061070

Fryirs, K. A. (2017). River sensitivity: A lost foundation concept in fluvial geomorphology. *Earth Surface Processes and Landforms*, *42*(1), 55–70. https://doi.org/10.1002/esp.3940

Fryirs, K. A., Wheaton, J. M., & Brierley, G. J. (2016). An approach for measuring confinement and assessing the influence of valley setting on river forms and processes. *Earth Surface Processes and Landforms*, *41*(5), 701–710. https://doi.org/10.1002/esp.3893

Geyman, E. C., Ke, Y., Magyar, J. S., Reahl, J. N., Soldano, V., Brown, N. D., et al. (2025). Scaling laws for sediment storage and turnover in river floodplains. *Science Advances*, *11*(15), eadu8574. https://doi.org/10.1126/sciadv.adu8574

Greenberg, E., Chadwick, A. J., Li, G. K., & Ganti, V. (2024). Quantifying channel mobility and floodplain reworking timescales across River planform morphologies. *Geophysical Research Letters*, *51*(12), e2024GL108537. https://doi.org/10.1029/2024GL108537

Grill, G., Lehner, B., Thieme, M., Geenen, B., Tickner, D., Antonelli, F., et al. (2019). Mapping the world's free-flowing rivers. *Nature*, *569*(7755), 215–221. https://doi.org/10.1038/s41586-019-1111-9

Henshaw, A. J., Gurnell, A. M., Bertoldi, W., & Drake, N. A. (2013). An assessment of the degree to which Landsat TM data can support the assessment of fluvial dynamics, as revealed by changes in vegetation extent and channel position, along a large river. *Geomorphology*, *202*, 74–85. https://doi.org/10.1016/j.geomorph.2013.01.011

Holušová, A., & Galia, T. (2025). Impact of river regulation on gravel bar decline and vegetation expansion over recent decades. *Catena*, *254*, 108910. https://doi.org/10.1016/j.catena.2025.108910

Hooke, J. M., & Yorke, L. (2011). Channel bar dynamics on multi-decadal timescales in an active meandering river. *Earth Surface Processes and Landforms*, *36*(14), 1910–1928. https://doi.org/10.1002/esp.2214

Hu, Y., Deng, J., Li, D., Lu, X., Zhou, J., Wang, C., & Li, Y. (2024). Shifted flood and ecology regimes due to channel bar greening and increased flow resistance in a large dammed River. *Geophysical Research Letters*, *51*(20), e2024GL110890. https://doi.org/10.1029/2024GL110890

Kleinhans, M. G., & Van Den Berg, J. H. (2011). River channel and bar patterns explained and predicted by an empirical and a physics-based method. *Earth Surface Processes and Landforms*, *36*(6), 721–738. https://doi.org/10.1002/esp.2090

Kryniecka, K., Magnuszewski, A., & Radecki-Pawlik, A. (2022). Sentinel-1 satellite radar images: A new source of information for Study of River channel dynamics on the lower Vistula River, Poland. *Remote Sensing*, *14*(5), 1056. https://doi.org/10.3390/rs14051056

Lamichhane, S., Karki, N., Pandey, V. P., Joshi, P., & Dawadi, S. (2025). Leveraging remote sensing for exploring climatic and hydro-geomorphic linkages to flooding: A case of Bagmati River in central Nepal. *River Research and Applications*, *41*(4), 953–965. https://doi.org/10.1002/rra.4413

Langhorst, T., & Pavelsky, T. (2023). Global observations of riverbank erosion and accretion from landsat imagery. *Journal of Geophysical Research: Earth Surface*, *128*(2), e2022JF006774. https://doi.org/10.1029/2022JF006774

Leenman, A., Greenberg, E., Moulds, S., Wortmann, M., Slater, L., & Ganti, V. (2025). Accelerated River mobility linked to water discharge variability. *Geophysical Research Letters*, *52*(2), e2024GL112899. https://doi.org/10.1029/2024GL112899

Leenman, A., Slater, L. J., Dadson, S. J., Wortmann, M., & Boothroyd, R. (2023). Quantifying the geomorphic effect of floods using satellite observations of River mobility. *Geophysical Research Letters*, *50*(16), e2023GL103875. https://doi.org/10.1029/2023GL103875

Li, Y., & Limaye, A. B. (2025). Coherent motion of channel threads in the braided Brahmaputra-Jamuna River. *Journal of Geophysical Research: Earth Surface*, *130*(6), e2024JF008196. https://doi.org/10.1029/2024JF008196

Llena, M., Vericat, D., Martínez-Casasnovas, J. A., & Smith, M. W. (2020). Geomorphic adjustments to multi-scale disturbances in a mountain river: A century of observations. *Catena*, *192*, 104584. https://doi.org/10.1016/j.catena.2020.104584

Maselli, V., Pellegrini, C., Del Bianco, F., Mercorella, A., Nones, M., Crose, L., et al. (2018). River morphodynamic evolution under dam-induced backwater: An example from the Po River (Italy). *Journal of Sedimentary Research*, *88*(10), 1190–1204. https://doi.org/10.2110/jsr.2018.61

McCabe, C. L., Matthaei, C. D., & Tonkin, J. D. (2025). The ecological benefits of more room for rivers. *Nature Water*, *3*(3), 260–270. https://doi.org/10.1038/s44221-025-00403-0

Monegaglia, F., Zolezzi, G., Güneralp, I., Henshaw, A. J., & Tubino, M. (2018). Automated extraction of meandering river morphodynamics from multitemporal remotely sensed data. *Environmental Modelling & Software*, *105*, 171–186. https://doi.org/10.1016/j.envsoft.2018.03.028

Montanari, A., Nguyen, H., Rubinetti, S., Ceola, S., Galelli, S., Rubino, A., & Zanchettin, D. (2023). Why the 2022 Po River drought is the worst in the past two centuries. *Science Advances*, *9*(32), eadg8304. https://doi.org/10.1126/sciadv.adg8304

Nardi, L., Campo, L., & Rinaldi, M. (2013). Quantification of riverbank erosion and application in risk analysis. *Natural Hazards*, *69*(1), 869–887. https://doi.org/10.1007/s11069-013-0741-8

Nones, M., Guerrero, M., Schippa, L., & Cavalieri, I. (2024). Remote sensing assessment of anthropogenic and climate variation effects on river channel morphology and vegetation: Impact of dry periods on a European piedmont river. *Earth Surface Processes and Landforms*, *49*(5), 1632–1652. https://doi.org/10.1002/esp.5791

Nyberg, B., Henstra, G., Gawthorpe, R. L., Ravnås, R., & Ahokas, J. (2023). Global scale analysis on the extent of river channel belts. *Nature Communications*, *14*(1), 2163. https://doi.org/10.1038/s41467-023-37852-8

O'Connor, J. E., Jones, M. A., & Haluska, T. L. (2003). Flood plain and channel dynamics of the Quinault and Queets Rivers, Washington, USA. *Geomorphology*, *51*(1–3), 31–59. https://doi.org/10.1016/S0169-555X(02)00324-0

Pavelsky, T. M., & Smith, L. C. (2008). RivWidth: A software tool for the calculation of River widths from remotely sensed imagery. *IEEE Geoscience and Remote Sensing Letters*, *5*(1), 70–73. https://doi.org/10.1109/LGRS.2007.908305

Pekel, J.-F., Cottam, A., Gorelick, N., & Belward, A. S. (2016). High-resolution mapping of global surface water and its long-term changes. *Nature*, *540*(7633), 418–422. https://doi.org/10.1038/nature20584

Piégay, H., Darby, S. E., Mosselman, E., & Surian, N. (2005). A review of techniques available for delimiting the erodible river corridor: A sustainable approach to managing bank erosion. *River Research and Applications*, *21*(7), 773–789. https://doi.org/10.1002/rra.881

Rice, S. P., Church, M., Wooldridge, C. L., & Hickin, E. J. (2009). Morphology and evolution of bars in a wandering gravel-bed river; lower Fraser river, British Columbia, Canada. *Sedimentology*, *56*(3), 709–736. https://doi.org/10.1111/j.1365-3091.2008.00994.x

Rinaldi, M., Gurnell, A. M., Del Tánago, M. G., Bussettini, M., & Hendriks, D. (2016). Classification of river morphology and hydrology to support management and restoration. *Aquatic Sciences*, *78*(1), 17–33. https://doi.org/10.1007/s00027-015-0438-z

Rowland, J. C., Shelef, E., Pope, P. A., Muss, J., Gangodagamage, C., Brumby, S. P., & Wilson, C. J. (2016). A morphology independent methodology for quantifying planview river change and characteristics from remotely sensed imagery. *Remote Sensing of Environment*, *184*, 212–228. https://doi.org/10.1016/j.rse.2016.07.005

Rusnák, M., Opravil, Š., Dunesme, S., Afzali, H., Rey, L., Parmentier, H., & Piégay, H. (2025). A channel shifting GIS toolbox for exploring floodplain dynamics through channel erosion and deposition. *Geomorphology*, *477*, 109688. https://doi.org/10.1016/j.geomorph.2025.109688

Schwenk, J., Khandelwal, A., Fratkin, M., Kumar, V., & Foufoula-Georgiou, E. (2017). High spatiotemporal resolution of river planform dynamics from Landsat: The RivMAP toolbox and results from the Ucayali River. *Earth and Space Science*, *4*(2), 46–75. https://doi.org/10.1002/2016EA000196

Surian, N. (1999). Channel changes due to river regulation: The case of the Piave River, Italy. *Earth Surface Processes and Landforms*, *24*(12), 1135–1151. https://doi.org/10.1002/(sici)1096-9837(199911)24:12<1135::aid-esp40>3.3.co;2-6

Sutfin, N. A., Rowland, J., Fratkin, M., Stauffer, S., Carroll, R., Brown, W., & Williams, K. H. (2020). River bank erosion and lateral accretion linked to hydrograph recession and flood duration in a mountainous snowmelt-dominated system. *Hydrology*. https://doi.org/10.1002/essoar.10503839.2

Wang, B., & Xu, Y. J. (2018). Dynamics of 30 large channel bars in the Lower Mississippi River in response to river engineering from 1985 to 2015. *Geomorphology*, *300*, 31–44. https://doi.org/10.1016/j.geomorph.2017.09.041

Ziliani, L., & Surian, N. (2012). Evolutionary trajectory of channel morphology and controlling factors in a large gravel-bed river. *Geomorphology*, *173–174*, 104–117. https://doi.org/10.1016/j.geomorph.2012.06.001